FREND Experiment Archive Interface Control Document (EAICD)

Annex 1

FREND Neutron Raw to Calibrated Data Processing Procedure

EXM-FR-ICD-IKI-0086 / Annex 1

Moscow, 2022

Table of Contents

1 Introduction

The FREND neutron telescope is installed onboard the Trace Gas Orbiter of the joint Russian-European mission ExoMars-2016 and has been mapping Mars from May 2018 to the present. The main purpose of the experiment is to assess the water content in the near-surface regolith at a depth of up to 1 m below the surface of Mars. This assessment is made by measuring the flux of epithermal neutrons from the orbit of Mars, which depends on the hydrogen atoms abundance in the soil. The document describes the conversion of the instrument's initial raw data into the neutron counting rate from Mars, which corresponds to the "calibrated data" product as it should be presented in the European Space Agency's Planetary Data Archive.

FREND is a nuclear physics complex instrument that includes a neutron telescope of the same name and a Liulin dosimeter (Mitrofanov et al., 2018). The neutron telescope maps the intrinsic neutron radiation of the Martian surface in the energy ranges from 0.4 eV to 500 keV (epithermal neutrons) and 500 keV to 15 MeV (fast neutrons). Processing of these data makes it possible to estimate the water content in the near-surface regolith of Mars at a depth of up to 1 meter with high spatial resolution. A brief description of the instrument and measurement techniques is presented in Chapter 2 of this document. Maps of water abundance are built based on a rather complex procedure for processing data from initial measurements consisting of three stages. At each stage of this procedure, official data "products" are created with an increasing degree of processing. These "products" are supplied to the Planetary Science Archive of the European Space Agency hereinafter referred to as the Archive, psa.esa.int) (see chapter 3).

The zero-level data "product" is created by converting the instrument's initial measurement data from the formats of its original telemetry information into the PDS4 (https://pds.nasa.gov/pds4/doc/sr/) format. These data are considered "raw" and are called FREND Raw Data (FRD).

The first processing level "product" contains count rate values in the detectors of the instrument for epithermal and fast neutrons emitted by Mars. The profiles are tagged with UTC World Time and can be correlated to the coordinates of the spacecraft in the near-Martian orbit. This "product" is called FREND Calibrated Data, or FCD. This document describes the procedures to convert the zero-level FRD data to the first-level FCD "product" for epithermal and fast neutron count rates (see Chapters 4 and 5).

The second-level data "product" is maps of the Mars surface containing values of a physical quantity called "suppression". This dimensionless quantity characterizes spatial variations of the neutron flux. It is calculated as the ratio of the average neutron count rate for a discrete surface area (pixel) and the reference value of the count rate in the Solis Planium Martian region, which, in accordance with previously obtained data, has the minimum water content for the entire planet equal to 2.78% by mass (Boynton et al., 2002). Estimates of suppression will be presented separately for the count rates of epithermal and fast neutrons. The advantage of using suppression values, defined as the ratio of count rates, is that they do not depend on the detectors' parameters. This product is called FREND Derived Data, or FDD (see Chapter 3). It will also be presented in the ESA Archive.

Based on the FDD suppression values, it is possible to estimate the mass fraction of water in the soil according the selected model of the regolith elemental composition and water distribution depth (Mitrofanov et al. 2022b). Specific details of the procedure for generating second-level FDD data will be described in a separate document.

Note also that this document focuses on the neutron data of the FREND instrument. Liulin dosimeter data processing is described in the Experiment Archive Interface Control Document EXM-FR-ICD-IKI-0086 directly. The document is available through the PSA website.

2 Brief description of the FREND instrument and measurement methodology

Nuclear physics techniques have been used successfully since the 1960s (Metzger et al., 1966; Trombka et al., 1970) to study the bodies of the Solar System, the Moon, Venus, Mercury, Mars, and asteroids to determine the elemental composition of the regolith, including the estimation of the hydrogen content, usually bound into water molecules (Boynton et al., 2002; Feldman et al., 2002; Mitrofanov et al., 2002; Mitrofanov et al., 2010; Sanin et al., 2017). Particles of galactic cosmic rays (GCR) collide with the nuclei of rock-forming elements in the near-surface layer of 1-2 meters thick, resulting in the formation of neutrons with energies of about several tens of MeV, diffusing in the matter of the celestial body due to numerous collisions with the nuclei of the main rock-forming elements. When colliding with such nuclei, the neutron energy changes little, in the proportion of m / M, where m and M are masses of the neutron and the nucleus, respectively. If hydrogen is present in the soil, then when colliding with hydrogen nuclei, protons, neutrons lose a significant share of energy comparable to the energy before the collision, since the mass of protons is equal to the mass of neutrons. Thus, if hydrogen is present in the substance of a celestial body, high-energy neutrons slow down much more efficiently. Some particles manage to leave the soil with energies greater than 0.4 eV. Such neutrons are usually called epithermal. Many other neutrons have time enough to slow down to thermal energies (thermalize) before leaving the surface. However, thermal neutrons can also be absorbed in nuclear capture reactions, that is why the magnitude of the thermal neutron flux emitted from the surface does not have an unambiguous relationship with the concentration of hydrogen atoms. Experience has shown that the measurement of the flux of epithermal neutrons leaving the surface is best suited for estimating the mass fraction of hydrogen in the substance, since their output flux depends only on the efficiency of the deceleration process.

It is known that the main hydrogen-containing chemical compound in the Martian regolith is water (Boynton et al., 2002; Feldman et al., 2002; Mitrofanov et al., 2002). In this regard, the amount of hydrogen in a substance is usually measured in equivalent percentages of the mass fraction of water (Water Equivalent Hydrogen, WEH). It has been established both experimentally and theoretically that the method of neutron sounding of the substance with epithermal particles is very sensitive to changes in the concentration of hydrogen: for example, a change in WEH in the regolith from 1 to 10% leads to a decrease in the flux of epithermal neutrons by almost 4 times (Drake et al., 1988; Masarik & Reedy, 1996). Details of the method for estimating the water mass fraction in the regolith based on measurements from the orbit of the proper neutron radiation of Mars, the Moon, and other celestial bodies are presented in (Litvak et al., 2012; Sanin et al., 2012).

Currently, the FREND instrument measures the neutron flux of Mars using two detection modules. The first module (Detection System for Epithermal Neutrons, or DSEN) includes four collimated proportional counters of epithermal neutrons in a cadmium shell HE1-HE4 filled with ^{3}He gas with the pressure of 6 atm. The second module (Detection System for Fast Neutrons, DSFN) includes a collimated detector SC made of stilbene for fast neutrons (Fig. 1).

Both the detection modules DSEN and the DSFN are structurally united by a common neutron collimator (Fig. 1). This collimator has five collimation openings. Four coaxial outer openings form the overall field of view of epithermal neutrons for DSEN counters, the central opening forms the field of view for the fast neutron detector. The collimator itself consists of external layer of high-density polyethylene and an inner layer of compressed ^{10}B powder. The outer and inner arrangement of the layers is determined separately for each collimation opening. Epithermal neutrons arriving from the outside are effectively slowed down in the outer layers of the collimator, and then are absorbed in the inner layer. Thus, only those neutrons that come within the fields of view of the collimation openings freely enter the detectors of the DSEN and DSFN modules.

The collimation efficiency of the instrument is well illustrated by the angular dependence of the count rate for epithermal neutrons and for fast neutrons (Fig. 2) (Malakhov et al., 2021). The width of the peaks of the angular sensitivity diagrams for the DSEN and DSFN modules is 14° (Half Width Half Maximum, HWHM). For observations from an orbit with an altitude of 400 km (the TGO orbit), these widths correspond to a spatial resolution on the planet surface with a radius of 60 km. (Mitrofanov et al., 2018)
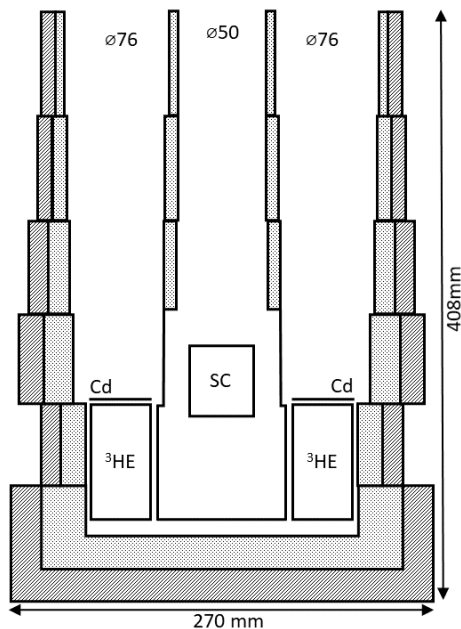
Figure 1 Diagram of FREND detectors and collimator. The HE1-HE4 helium counters of the DSEN module and the SC scintillation detector of the DSFN module inside the collimator limiting their field of view are shown. The collimator consists of layers of high-pressure polyethylene outside (hatches) and 10V powder inside (dots).

Figure 2 Angular diagram of the sensitivity of collimated detectors HE1-HE4 of the DSEN module and SC of the DSFN module of FREND shows a significant suppression of the neutron flux outside the collimator field of view, at angles of 14° and higher.

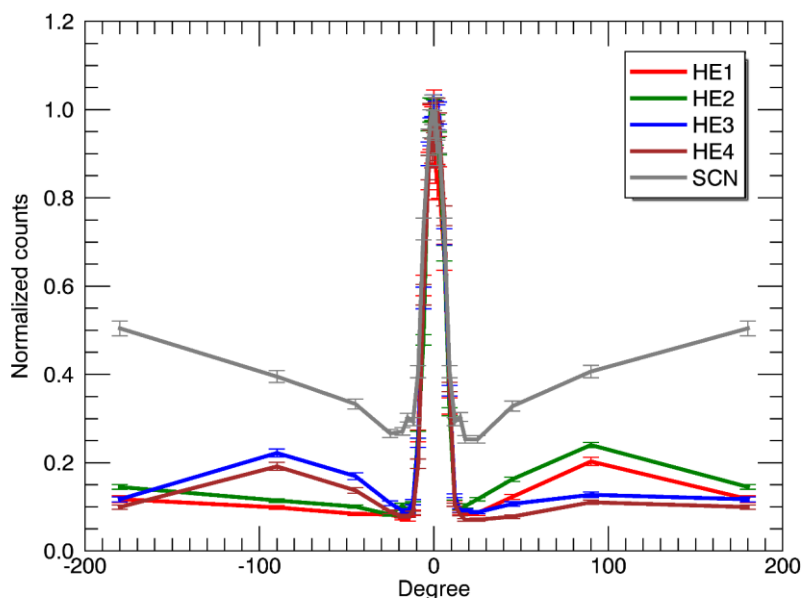The TGO spacecraft flies in a circular orbit of Mars at an altitude of about 400 km. The inclination of the orbit is 74 °, that is why the neutron mapping of the planet occurs in the latitudinal belt from 74 ° N to 74 ° S. During the orbital flight, the FREND instrument is usually turned on and constantly measures the neutron flux. It should be noted that the axis of the fields of view of DSEN and DSFN regularly turns away from the direction to the nadir for other measurements, so not all of the resulting FREND measurement data are used for neutron mapping. In addition, the detectors of the instrument are turned off in the case when the conditions of the space flight do not allow to perform measurements: during propulsion operations, during the eclipse of Mars by the Sun and in other similar cases. The method of filtering the FREND data is described in Chapter 4. The total time loss of neutron mapping is about 32% of the total time of orbital measurements.

3 Description of data types in the Archive

In accordance with the practice established for space experiments of ESA projects, all the results obtained are publicly available in the Archive (psa.esa.int). The structure of the Archive involves the storage of both the initial measurement data and the results of their processing. At the same time, the so-called "products" of data at different levels of their processing allow researchers to use them for their own purposes using both procedures proposed by the authors of the experiment and procedures of their own design, without having special knowledge about the instrument from which they were obtained.

The archive is organized on the basis of a hierarchy of data types in accordance with their processing levels (see Table 1). Only neutron scientific data products are described in this Annex and thus in Table 1. All types of products are listed in the EAICD's main text, see Section 3.2.

Table 1 FREND Data Types and Their Hierarchy in the ESA Archive

Data type name	Description of the data type	Description of FREND data
RAW Neutron Science Data (FREND Raw Data, FRD)	The initial data of the instrument in the form in which they are obtained in the instrument telemetry without any transformations other than formatting.	The initial data of the instrument after conversion to the standard Archive PDS4 format (FRD "product") are presented. They contain time profiles of samples relative to on-board and Universal Time with a resolution of 5 seconds in 16 energy channels of the detectors and service telemetry data of the instrument with a time resolution of 30 seconds (description of data formats, as well as the data themselves, are available on the archive website, psa.esa.int).
Calibrated Neutron Science Data (FREND Calibrated Data, FCD)	Data of the first level processing: the initial data in the PDS4 format were converted into values presented in generally accepted physical units after applying calibration curves and other necessary corrections to them in order to take into account technical features of the instrument.	Profiles of the count rate of epithermal and fast neutrons from Mars with a resolution of 5 seconds relative to Universal Time are presented for the DSEN and DSFN modules (FCD "product"). The structure of the FCD data is described in Chapter 4. FRD data processing methods for obtaining FCD data are described in Chapter 5 of this document.
Derived Neutron Science Data (FREND Derived Data, FDD)	Data obtained after processing calibrated data is the final product of the space experiment. As a rule, to obtain data of this level, it is necessary to use various mathematical processing procedures and numerical models.	Maps of epithermal and fast neutron fluxes suppression are presented in the form of two-dimensional arrays for elements of Mars surface with a size of 1° x 1° (pixels) within the latitudinal belt from 75° S to 75° N (FDD "product"). The method of constructing these maps will be described in future documents in conjunction with the supply of data of this level to the Archive.

During the calibration phase of the interplanetary flight from 16.04.2016 to 27.04.2018, it was discovered that sporadic noises are observed in the HE1 counter, probably associated with micro-discharges in the high-voltage unit. It was decided to transfer this counter to the reserve mode in order to prevent possible damage to the integrated circuits of the logical-digital node of the instrument and to provide this counter with additional time for restoration of high-voltage insulation. Three HE2-HE4 and SC detector have been operating normally since the first switch-on. In view of the above, the FRD data "product" contains blocks of data of all detectors, including "empty" blocks for the HE1 detector, while in generation of higher data "products", FRD and FDD, only HE2-HE4 and SC measurements are used.

4 Physical description of measurements of the FREND instrument

4.1 Physical conditions for detecting epithermal neutrons in the DSEN module

The HE1-HE4 proportional counters of the DSEN module are filled with ^{3}He gas and have a cylindrical shape with an active volume size of 78 mm (height) by 50.8 mm (diameter) and a pressure of 6 atmospheres. Their energy sensitivity range for neutrons has an upper limit of 500 keV. On the side of the collimator opening, the detectors are covered with cadmium plates 1 mm thick (see Fig. 1). The lower limit of the energy sensitivity range corresponds to the upper energy threshold of the neutron absorption cross-section by cadmium of about 0.4 eV.

Measurements of counts in the counters are carried out in 16 energy channels with a time resolution of 5 seconds. An example of spectra of counts measured in Martian orbit by HE2-HE4 counters per day of measurements is presented in Fig. 3. It should be noted that the energy distribution of counts in the DSEN module counters does not characterize the energy spectrum of neutrons registered in it, since the counts in the detectors arise not only when neutrons are registered, but also because of the passage through them of charged particles of galactic cosmic rays (GCR).

The FRD/EN data "product" of measurements in the DSEN module is presented as a complete initial energy spectrum of counts in 16 spectral channels of HE2 – HE4 counters (Fig. 3).
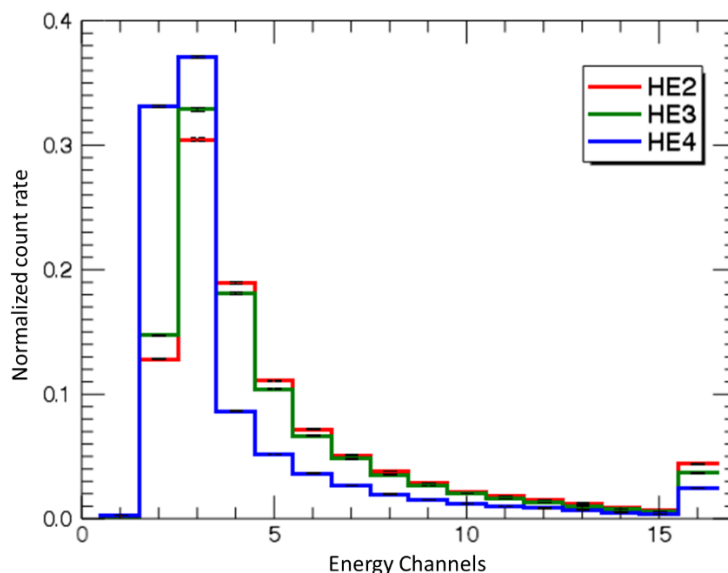

Figure 3 The count spectra for the HE2-HE4 epithermal neutron counters of the DSEN module, measured in the Martian orbit, show the contribution of charged particles, which have a characteristic power-law spectrum shape, in the lower channels. The spectra are normalized by amplitude at full counting rate

Counts from neutrons arise due to the nuclear reaction of neutron capture by the ^{3}He nucleus with the formation of a proton and a triton. This reaction results in the release of an energy of 764 keV, which is distributed between the proton and the triton in a ratio of 573 and 191 keV, respectively. Counts energy spectra when registering neutrons with energies << 764 keV do not depend on the energy of the neutron.

Figure 4 shows the neutron registration spectra of HE2 – HE4 counters measured during ground physical calibrations of the DSEN module. The efficiency of these counters decreases for neutrons with energies of about 500 keV, therefore, the measured count spectra are determined only by the conditions of ionization of helium atoms by proton and triton formed in the nuclear reaction in the active volume of the counter, and also by the conditions of charge collection in the electrostatic field of the counter.

The right peaks of the spectra in channels 8 – 10 correspond to the complete absorption of all the released energy of 764 keV in the active volume, when both particles completely lose their energy through ionization. The counts in channels 4 – 7 correspond to cases of partial absorption of the released energy due to protons escaping the active volume prior to the complete loss of their energy through ionization. The counts in channels 2-3 of the left peak correspond to the energy release from tritons, when the formed protons almost immediately leave the active volume without losing energy through ionization. Generally speaking, this form of the count spectra can change depending on the configuration of the electrostatic field in the volume of counters. This property of counters was manifested during measurements in space (see later in this section).
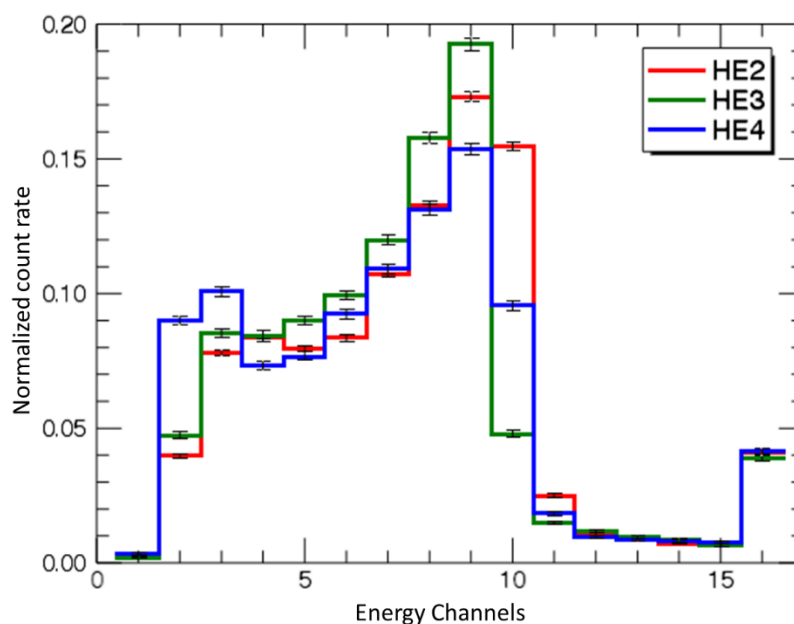

Figure 4 The count spectra for the HE2-HE4 epithermal neutron counters of the DSEN module, measured during ground calibrations using a reference neutron source, have a classical form of the neutron spectrum. The spectra are normalized by amplitude at full counting rate.

Fig. 3 shows that when working in space, counts from charged particles dominate in the lower energy channels, the characteristic spectrum of which differs significantly from the spectrum of counts from neutrons shown in Fig. 4. Given the predominance of the contribution of charged GCR particles to the counts in channels 1 – 5 and the effect of the amplitude discriminator, the measurement data of the DSEN module counters in these channels are completely excluded from consideration. The data for the counts in the last integral channel 16 are also excluded from consideration, since it is known from physical calibrations that the reactions from the detection of epithermal and thermal neutrons do not contribute to this channel.

At the first stage of processing, each measured count spectrum in channels 6 – 15 for HE2 – HE4 counters was presented with the test model in the form of the sum of the neutron count spectra $Sp_{cal} + Sp_{cor}(E)$ with the free parameter A_N and the power-law spectrum of counts from GCR particles $Sp_{GCR}(E)$ with exponent P_{GCR} and amplitude A_{GCR} as free parameters. Based on the application of the Pearson criterion with the residual functional corresponding to the χ^2 distribution, the values of the free parameters {A_N, P_{GCR} and A_{GCR}} were determined, for which the best agreement of the measured and model counts is achieved. It was found that the values of the functional do not reach the values at which the difference between the experiment and the model could be explained by statistical fluctuations. It turned out that for a large set of measurements, the values of residuals for each channel practically do not change. It was suggested that the appearance of constant values of residuals in the spectral channels of detectors HE2 - HE4 is associated with a change in the shape of the neutron counts spectra measured in space conditions relative to the spectra measured in ground calibrations. It can be assumed that these changes occur because of the changes in the lines of the electrostatic field in the active volume of the counters due to the accumulation of charges on the inner surface under the influence of GCR. It was shown that the addition of this spectral residual $Sp_{cor}(E)$ to the ground calibration spectrum $Sp_{cal}(E)$ leads to a good statistical agreement with the experimental data.

Thus, all the initial measurement data in the HE2 – HE4 counters, based on the procedure described above, are decomposed into spectral components of counts from neutrons and from GCR particles. The value of the component for neutron counts corresponds to A_N ($Sp_{cal}(E) + Sp_{cor}(E)$). The value of the component for GCR particle counts corresponds to $Sp_{GCR}(E)$ with a P_{GCR} power and an amplitude of A_{GCR}. The values of A_N, A_{GCR} and P_{GCR} shall be determined by the criterion of best agreement (see Section 5.4).

4.2 Physical conditions for detecting fast neutrons in the DSFN module

Fast neutrons are detected by a stilbene scintillation detector of the DSFN module (Fig. 1). The registration reaction is the knocking out of a proton by an energetic neutron from the structure of the scintillator and with the transfer of significant energy of the incident neutron to it. The amount of transferred energy depends on the angle between the directions of dispersal of the proton and the neutron after collision in the center of mass of the two particles. At an angle of 180°, the proton acquires all the energy of the neutron, at an angle of 0° the energy transmitted to the proton is 0. The free proton in stilbene causes scintillation radiation, the total intensity of which is proportional to the energy left by the proton in the scintillator substance. Thus, the energy range of the detector of the DSFN module starts from the minimum value of the light output from the scintillator recorded by PMT and goes up to the maximum value corresponding to the crystal transparency properties for energetic neutrons.

The DSFN module detector performs measurements with a cylindrical stilbene crystal, 36 mm (height) by 36 mm (diameter). A crystal of this size registers neutrons with energies up to 15 MeV. This value can be considered the upper limit of the energy range. The detector uses a PMT manufactured by Hamamatsu. The lower limit of its light output corresponds to an energy release of about 500 keV. This value can be considered as the lower limit of the DSFN energy range.

The DSFN module does not have anti-coincidence protection against registration of counts from charged GCR particles. To separate counts from neutrons and counts from energetic charged particles, a method of counts selection is used. The stilbene crystal is surrounded on all sides by a 5 mm plastic shield in which scintillation flashes occur when photons are registered and when GCR particles pass through. Both volumes, crystal and plastic, are scanned by one PMT, while the separation of pulses into neutron and charged particles is carried out by the analog electronics of the detector through analysis of the amplitude, shape and duration of pulses in the PMT. The thicknesses of the plastic detector and the stilbene crystal are selected in such a way that the shapes of the PMT signals can be unambiguously distinguished. (Malakhov et al., 2022). Thus, at the output of the SC detector, two data signals are formed - SCN for counts from fast neutrons and SCG for counts from charged particles and gamma photons.

The FRD data "product" with neutron measurements in the DSFN module is represented as an count energy spectrum in 16 spectral channels for the SCN signal (Fig. 4). The optimal signal-to-noise ratio is observed in channels 1–7: during ground testing, when the FREND instrument was irradiated with high-energy protons, a significant signal from protons was observed in channels 8–16, which does not allow use of these channels to analyze the neutron signal from Mars. The physical meaning of the task of creating a higher-level data "product" for fast neutrons measured by the DSFN module (FCD/FN) is to isolate in the full SCN counts contained in the FRD product, the part of the fast neutrons counts that are emitted by Mars. Chapter 5 below shows that the availability of the measurement data at different stages of flight and understanding of the origin of various components of the measured count spectra can successfully solve this problem.
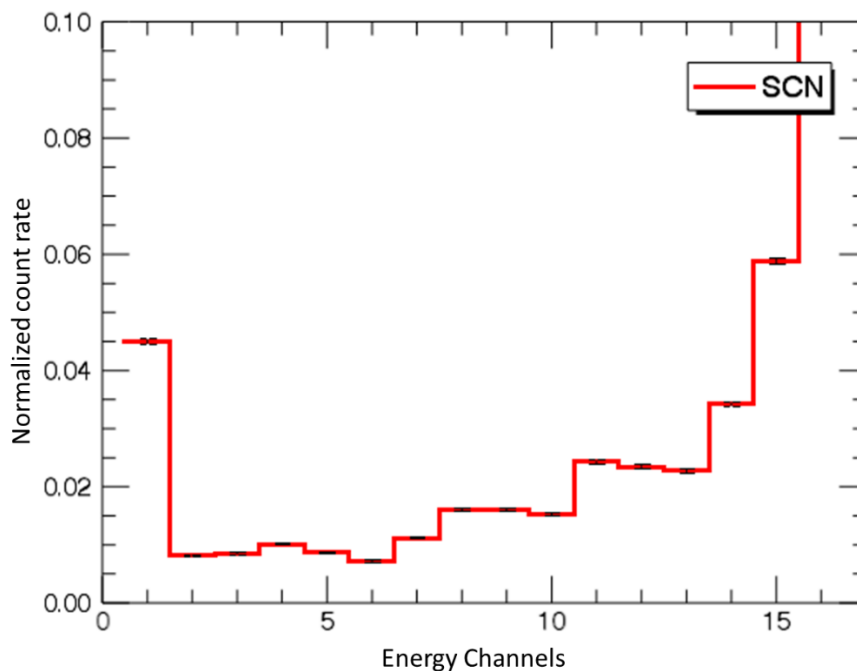

Figure 5 The count spectrum of the SCN fast neutron signal measured by the SC detector of the DSFN module

5 Methodology for processing initial data to obtain first-level data

As mentioned above, the original FRD/EN and FRD/FN data contain 5-second time profiles of the count spectra of the DSEN and DSFN detectors in 16 energy channels. In order to obtain the first level "product", FCD (calibrated data), the following procedures are performed:

- preparation of initial data suitable for neutron mapping of Mars;
- adjustment of the initial data, taking into account the instability of the efficiencies of the detectors, to - take into account the variability of the GCR flux;
- extraction of the Mars neutron count rate from the DSEN module HE2 − HE4 detectors total count rate and the DSFN module SC detector SCN total count rate.

The following sections describe how to perform these procedures.

5.1 Effects of raw data variations due to changes in the efficiency of DSEN and DSFN detectors

Proportional counters of epithermal neutrons HE2 − HE4 of the DSEN detection module reach the level of maximum efficiency only after a long time after applying high voltage to them, up to several weeks (Fig. 6).

The reason of this instability is the change in the configuration of the electrostatic field in the active volume of the detectors when they are irradiated by energetic particles of the GCR. This effect can be called variations effect of in the count rate of HE detectors from the saturation of efficiency (VE/SE/HE).
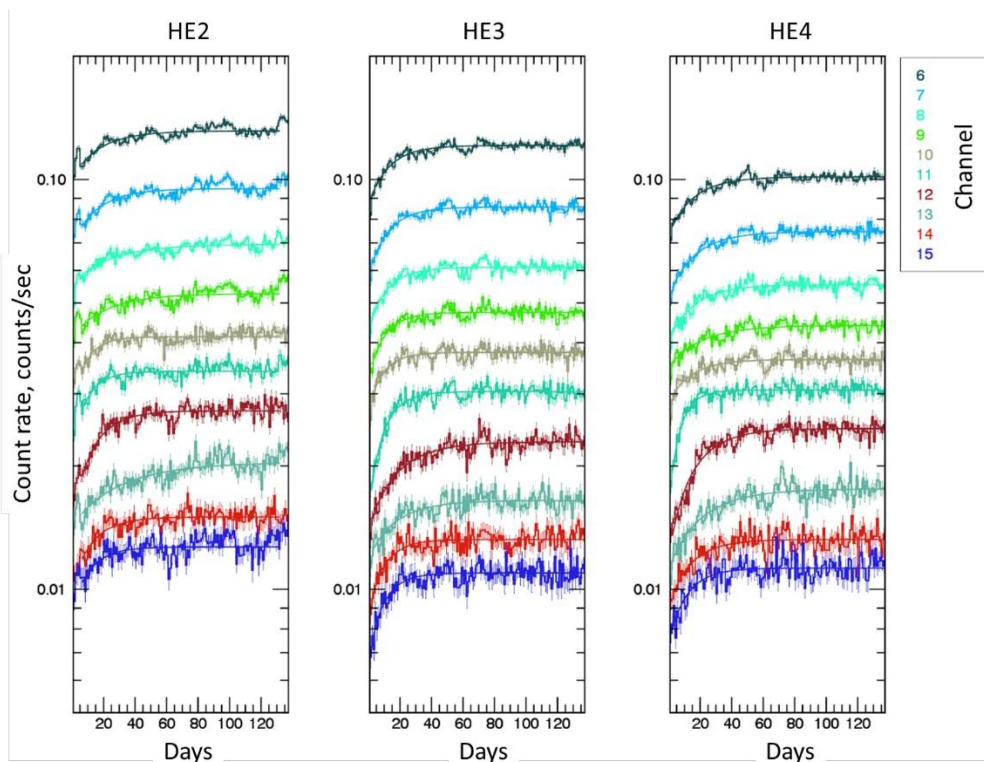

Figure 6 Change in the count rate of the DSEN detectors associated with reaching the full efficiency (VE/SE/HE) after activation. As an example, counting rates averaged over 1 day in spectral channels 1-16 (shown in colors) of detectors HE2 – HE4 of the DSEN module are shown after switch on on April 27, 2018. Smooth curves show the approximating functions used for correction.

The SC detector of the DSFN module also changes its effectiveness over time. The decrease in the efficiency of the detector is due to the slow degradation of the PMT under the influence of a constantly operating GCR flux (Fig. 7). It should be noted that the effect of variations in the counting rate of the SC detector from the decrease in efficiency (VE/DE/SC) does not depend on the spectral channel - it can be described by a single law which does not change the count rate ratio before/after degradation in different spectral channels of the SC detector.
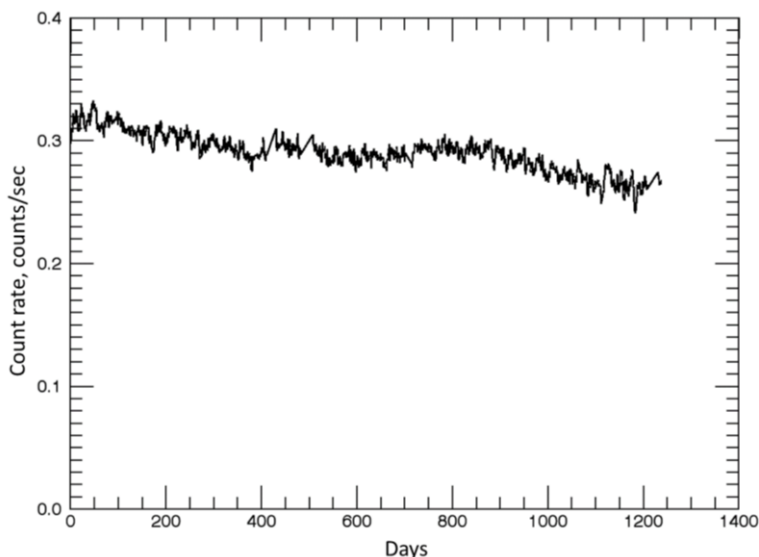
Figure 7 Change in the count rate of the SC detector of the DSFN module associated with a decrease in efficiency (VE/DE/SC) in channels 1-7. The trend is shown since the beginning of the mission on April 27, 2018.

Thus, the raw measurement data need to be adjusted to eliminate variability due to effects VE/SE/HE for DSEN and VE/DE/SC for DSFN. It should be noted that in addition to the long-period variability due to effects related to the behavior of the detectors, the raw measurement data also contain the variability of the GCR particles flux that causes the neutron radiation registered by both modules of the telescope, DSEN and DSFN. Data measured during periods of rapid variation in the GCR flux (tens of hours) cannot be corrected and has to be excluded from further processing (see section 5.3 below). The remaining bulk of the measurement data is accumulated under the conditions of long-period GCR variations, and thus needs to be corrected to eliminate variability due to the effect of variations from GCR variability (VE/GCR) (see 5.4 below).

It should be noted that it is not possible to correct the HE2 – HE4 data to exclude both effects, VE/SE/HE and VE/GCR, within the same procedure, since in the first case a separate selection of correction coefficients is required for each spectral channel of each counter separately. The description of the data adjustment procedure to exclude the effect of EV/NE/HE is presented below in section 5.2. On the contrary, to correct the initial data of the SC detector to eliminate both effects of VE/DE/SC and VE/GCR, a single procedure can be applied based on the procedure for correcting the data of HE2-HE4 detectors with respect to EV/GCR (see Section 5.4).

5.2 Correction of HE2-HE4 data relative to the effect of saturation of efficiency

Figure 6 shows that the exponential function approximation is best suited to correct for the efficiency. Obviously, in order to correct the initial data of the HE2 – HE4 detectors for an increase in efficiency, it is necessary to accumulate data for several weeks – a satisfactory approximation of the saturatuib law can be obtained if there is a long "plateau" in the data, when the registration efficiency becomes constant.

For each energy channel of the count spectra of each HE2 – HE4 detector of the DSEN module, an approximating function is selected:

$$F = A \cdot [1 - e^{B \cdot (t - C)}] \qquad (1)$$

where A, B, C are free parameters for finding the best approximating function, t is the time of measurement.

The best values for these parameters are selected based on the criterion of the model's agreement with the measurement data. In this case, formal statistical criteria for assessing the approximation quality does not

apply, since the counting profile, in addition to statistical fluctuations, also has variability due to short-period variations in the GCR flux (see section 5.4 below). It should be noted, however, that in order to estimate the best values of the parameters of the approximation function (1), measurement data are used for such periods of time when the GCR flux differs little from the average in the full time interval for which the data should be corrected (i.e. the GCR variation is mild). To verify the quality of the correction of the data to the VESE/HE effect, estimates of the data dispersion from the average reference profile were made, corrected for both the VE/SE/HE and VE/GCR effects. These estimates were made both for the time periods immediately after the activation of the HE2- HE4 detectors, where data were adjusted, and for the periods of time, when the detectors saturation has completed and no correction of the data for VE/SE/HE effect was required (see section 5.4 below). It was shown that the values of mean dispersions for such time periods practically coincide . This confirms that the proposed adjustment procedure does not contribute further to the errors of the measurement data.

Thus, it can be affirmed that the correction of data for specific time intervals after turning the instrument on showed that it allows almost completely to eliminate the VE/SE/HE effect (Fig. 8). Statistical errors of the count values after the correction is applied are estimated based on the errors of the raw measured count values.

It should be noted, however, that the need to adjust the raw DSEN module data during time intervals after each activation, considering the most conservative approach to orbital mapping, leaves doubts on use of such corrected data. It was decided to tag the first level of FCD/EN data that had undergone such correction. Thus the question of using these data to generate a neutron flux map is left to the discretion of each researcher.
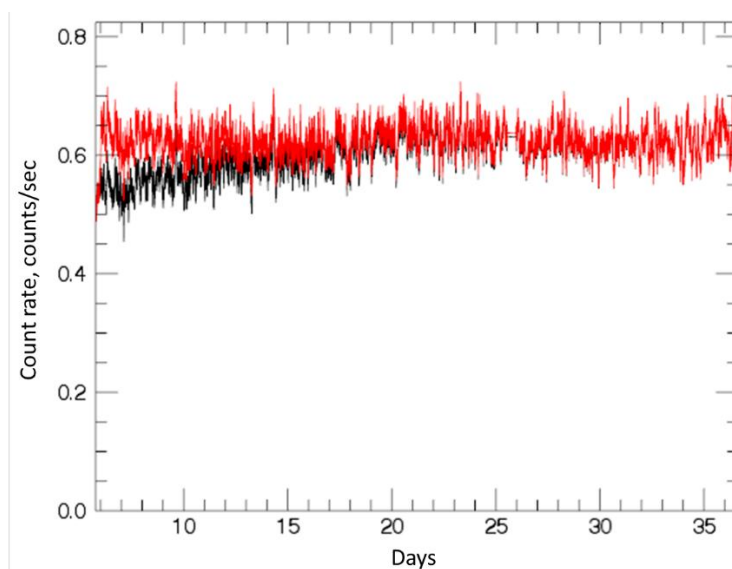

Figure 8 Example of data correction for detector efficiency after switching on. Black graph corresponds to the measured count rate in channel 6 of the HE2 detector (selected as an example). Red graph is the count rate after adjusting for the effect of the efficiency increase of the the detector. The figure shows data, smoothed with a period of 2 hours.

5.3 Reducing the volume of raw FRD data to create the first-level FCD data suitable for mapping

The flight time of TGO in the mapping orbit from 27.04.2021 to the date of preparation of this document, 04.11.2021 is 1289 days. The total measurement time suitable for mapping during this period is 821 days. This difference is due to the fact that parts of measurements that are unsuitable for mapping have to be excluded from the full FRD data set (see Table 2). When creating the FCD data product, special labels are assigned to all measurements (Table 2), thus, the decision to use them for mapping can be made by each

user independently. These labels are stored as separate fields of the Archive dataset and can be linked to each individual measurement.

Firstly, neutron mapping of Mars is carried out by pointing the axis of the instrument's field of view into the nadir. Measurement data in which the angle of deviation from the nadir exceeds 1° (off-nadir condition) should be excluded from consideration. Total measurement time in off-nadir conditions was 333 days.

Secondly, the data obtained during solar flares and solar proton events should be excluded from the full amount, since additional fluxes of the Sun energetic charged particles affect the count rate in the FREND detectors.

Thirdly, all measurements for the first 2-5 days after each switching on of the instrument are excluded from the analysis, since after switching on the temperature of the secondary power sources increases quite rapidly, which causes a change in the energy channels of the detectors and, as a consequence, a change in their count rates (see section 5.2).

Fourthly, irregular periods of count rate increase were discovered in the HE2 detector data, which are not supported by measurements of the HE3-HE4 detectors. Such data are similarly excluded from consideration.

Finally, it should be borne in mind that the FREND instrument is turned off in case of the spacecraft requirements - for example, during periods of active maneuvering, lack of communication with the spacecraft, or other events (76 days).

Table 2 shows the proportion of labeled FRD level data for each case.

Table 2 The portion of data marked as unusable in the FCD product

Data property	Data share (%) for this type	Label field in the archive
Instrument Data for all time of operation in the period from 27.04.2021 to 04.11.2021	100	
Off-nadir data	26	OFF_NADIR
Data collected within 2-6 days after activation	2	BAD_EFFICIENCY
Data obtained under the conditions of the active Sun	0	SOLAR
Data corrected to eliminate the effect of efficiency saturation	32	CORRECTED_EFFICIENCY
Data with a deviation of the HE2 count rate from the HE3-HE4 count rate.	4	BAD_HE2
Data suitable for creating FCD including the data that were corrected for efficiancy saturation	68	GOOD_TO_MAP (contains all data except OFF-NADIR, BAD_EFFICIENCY, SOLAR and BAD_HE2)
Data suitable for creating FCD excluding the data that were corrected for efficiency saturation	36	Not tagged in the archive, matches all measurements marked with GOOD_TO_MAP tags and not marked with CORRECTED_EFFICIENCY

Thus, the portions of DSEN module FRD/EN data that can be used to create FCD/EN are 68% and 36% depending on the inclusion or exclusion of data adjusted for efficiency saturation. Similarly, the proportion of DSFN module FRD/FN data that can be used to create FCD/ FN, is 72%.

5.4 Correction of the raw FRD data to exclude their dependence on GCR variations

Mars neutron flux mapping can be successful only if the FCD data with Mars neutron count rate do not have any variability other than the variability due to variations in neutron flux for different regions of the planet. It is known that charged GCR particles are the cause of neutron radiation from Mars (see Section 2) and that the GCR flux changes due to the influence of interplanetary field inhomogeneities on these particles .

Therefore, for mapping of Mars neutron radiation , the effect of GCR variability (VE/GCR) must be excluded from the raw FRD measurements.

The raw FRD orbital measurements data to be corrected is the time series of the average count spectra of the HE2 - HE4 detectors, measured in a given reference area on the surface of Mars for a set period of time. The averaging conditions shall ensure that the averaged values are constant if the GCR flux is constant. In that case the observed changes in these values indicate a change in the average GCR flux during the averaging period. It was decided to choose a latitude band ranging from 40 S to 40 N as the reference area on the surface, and 1 Earth Day as the time period for averaging. During this time, the projection of the spacecraft's orbit uniformly covers the entire latitudinal band of the planet's surface; therefore, with a constant GCR flux, the average neutron flux should remain constant.

To adjust the detector HE2 – HE4 data in order to eliminate the VE/GCR effect , the averaged count spectra measured for the specified latitudinal band within 1 day should be divided into components of counts from charged particles and from neutrons. Generally speaking, the total count spectrum is also proportional to the average flux rate of the GCR, so its variations could also be used directly to estimate correction coefficients. However, in this case, a systematic error may occur due to the presence of contributions from measurements in off-nadir conditions in the data. The contribution of such measurements does not affect the size of the count component from cosmic rays, while the count component from the Martian neutrons flux can change depending on the areas of the surface and on the off-nadir angle. Therefore, the estimation of VE/GCR correction coefficients is based on the averaged GCR particles spectra component.

It has been shown above (see section 4.1) that the count spectra of helium counters in channels 6–15 (Fig. 3) are well described by the sum of two components: the energy spectrum of neutron counts and the energy spectrum of the counts from the GCR particles. Accordingly, for each detector HE2, HE3 and HE4, each count spectra averaged over a set of days of Orbital measurements can be split into these two components. This splitting is performed for spectral channels $6 - 15$ in which the contribution of neutrons predominates (see section 4.1). To perform this splitting, the values of free parameters A_N, A_{GCR} and P_{GCR} are evaluated such that they ensure a minimum of function:

$$F = \sum_{i=6}^{15} \frac{(S_i - S_i^*)^2}{\sigma_i} \qquad (2)$$

where i is the number of the spectral channel from 6 to 15; S_i - measured count values; $S_i^* = S_p + S_n$ are the sum   of the values for the model count spectra of particles and neutrons; error $\sigma_i = (\Delta S_i)^2 + (\Delta S_i^*)^2 \approx (\Delta S_i)^2$ is mainly determined by the dispersion of the measured count rate. The error of the calibration neutron spectrum and the inaccuracy of the shape of the particle spectrum can be neglected, since the statistical certainty of calibration spectrum measurements is many times greater than the certainty of the spectrum S_i, and the particles model spectrum does not have an error by definition.

Figure 9 shows an example of the splitting of the spectrum measured during a day into particle and neutron components in each of the three HE2-HE4 detectors..
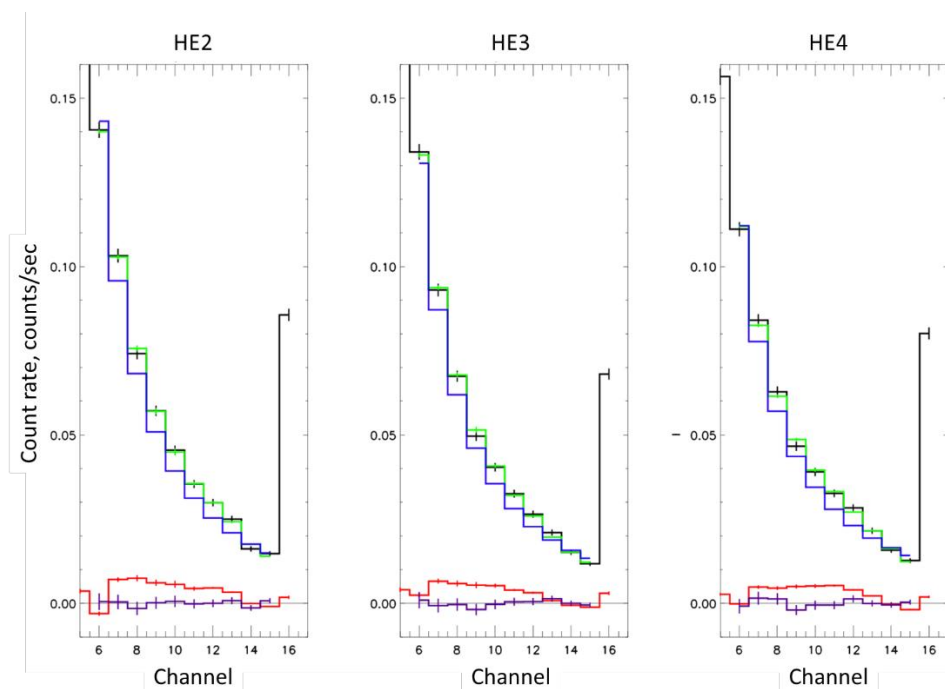
Figure 9 Splitting of the spectrum of detectors HE2-HE4 of the DSEN module into components. The measured spectrum of particles (black) splits into two components - particles (blue) and neutrons (red). The green spectrum is the sum of red and blue, violet - residual (difference between the measured black and model green spectra).

To obtain the correction coefficient for the FRD data relative to the VE/GCR effect, the integral of the charged particles spectral component in each detector and in each day is divided by its value on the very first day of orbital measurements (corresponds to May 2, 2018 – the first day of FREND measurements in Martian orbit, suitable for mapping in accordance with section 5.2). As a result, for each current day, the cosmic ray normalization factors K_{GCR} for each of the three detectors are obtained (shown in Figure 10). The variability profiles of the correction coefficients relative to VE/GCR for the three counters HE2 - H4 are in good agreement. These profiles reflect the physical variability of the GCR flux over the entire observation time.

These coefficients for each detector are used to normalize the detector count rates for each day during mapping time: the coefficient is applied to the sum of channels # 6-15 in raw detector count rates. As a result of this correction, the original FRD data are "cleared" of the variability associated with the variation of GCR and are brought to the intensity of the GCR as of May 2, 2018.

After carrying out this correction of the HE2 – HE4 data to VE/GCR effect, a quality check of the correction of these data with respect to the VE/SE/HE effect was performed (see section 5.3 above). Two total observation periods of the same duration of about 60 days were selected: the first period included time intervals after the activation of the HE2 - HE4 detectors, which were adjusted for VE/SE/HE. The second period included intervals of measurements with detectors in the state of constant maximum saturation. The mean dispersion values for these two periods were 0.28 and 0.25. From the good agreement between these two values, it follows that the data correction for the VE/SE/HE effect does not add additional errors and practically does not degrade the quality of the DSEN measurement data.

It was noted above that the correction of the DSFN module SC detector data with respect to the VE/DE/SC and VE/GCR effects can be performed in a single procedure, since the correction coefficients do not require an estimate for each spectral channel separately. For this, a similar procedure is applied to normalize all data to the level of GCR as of May 2, 2018. Correction coefficients for each day's average values are obtained from fast neutrons measurements in the latitudinal belt of -40 to +40 degrees.
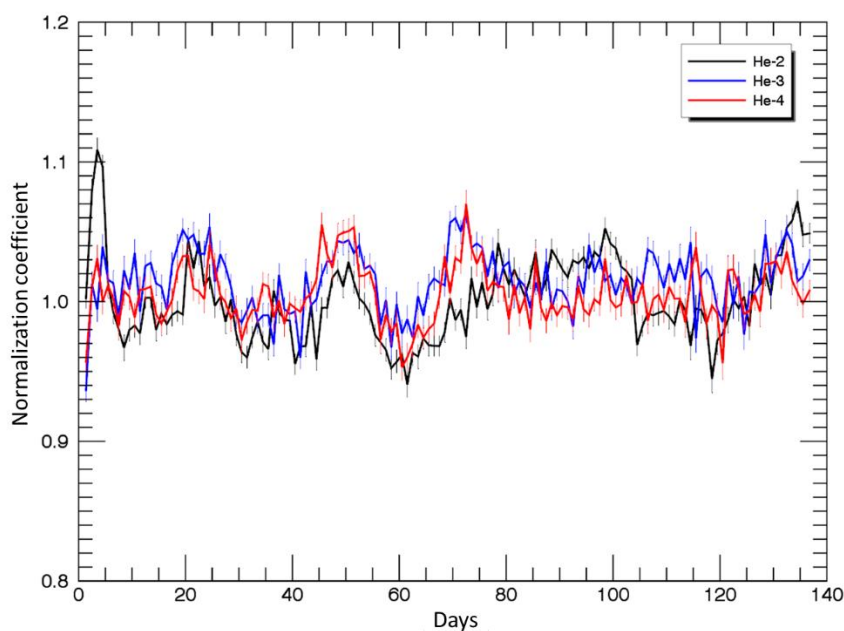
Figure 10 Correction coefficients relative to the variations effect in GCR (VE/GCR) for the HE2-HE4 detectors of the DSEN module coincide well and reflect the variability of the GCR fluxes

5.5 FCD/EN and FCD/FN data: fluxes of epithermal and fast neutrons from Mars

The baseline data for estimates of neutron count rate from Mars are the counting rate time profiles of the SDEN and SDFN detectors, from which the data for time intervals unsuitable for orbital mapping are excluded (see section 5.3) and which are corrected for detector efficiency and GCR variability (see sections 5.2 and 5.4). These baseline data, presented in the format of count rates (counts/sec), are the sums of the two components:

$$C_{tot} = C_{sig} + C_{bgd} \qquad (3)$$

where C_{tot} is the full count rate, C_{sig} is the Mars neutron count rate , which is a "useful signal" for the purposes of the FREND experiment, C_{bgd} is the background count rate from charged GCR particles and from secondary spacecraft (SC) neutrons that arise in the SC structure under the influence of GCR.

To create calibrated data products of FCD/EN and FCD/FN (see Table 1), it is necessary to extract the C_sig component, which contains information about the variability of the neutron flux from the planet's surface, from C_tot,.

To assess the background C_{bgd} from the spacecraft, we use data measured in the highly elliptical orbit, on which FREND has been working from November 2016 to March 2017, before the beginning of aerobraking and the nominal circular orbit. In the apocenter of such an orbit, at a distance of 90,000 kilometers from Mars, the instrument recorded only counts from charged GCR particles and from secondary SC neutrons formed under the influence of GCR. The C_{sig} signal component is completely absent in the total count rate C_{tot} of the instrument.

For 24 apocenters of a highly elliptical orbit, average values of total count rate in the conditions of interplanetary space were obtained. Similarly to the technique described in Section 5.4, these values were

adjusted to the GCR intensity at the start of the scientific mission on May 2, 2018. As a result, the values presented in Table 3 (line 1) were obtained for epithermal and fast neutron fluxes.

Table 3 Estimation of the Background Count Rate

#	Measured values	HE2	HE3	HE4	SC
1	Values of the full count rate in apocenter (count/sec)	0.644	0.588	0.511	0.338
2	Estimation of background count rate C_{bgd} in orbit (count/sec)	0,465	0,424	0,369	0,244
3	Values of the full orbital count rate (count/sec)	0,498	0,442	0,398	0,323
4	Values of the neutron count rate from Mars in orbit (count/sec)	0,033	0,018	0,030	0,079

It is natural to assume that when the SC approaches Mars, its own neutron background decreases proportionally to the coefficient:

$$K_{SA} = \frac{(4\pi - \Omega_{SA})}{4\pi} \tag{4}$$

where Ω_{SA} is the magnitude of the solid angle of Mars, depending on the altitude of the SC's orbit. Similarly, the count rate from charged particles decreases. Therefore, to estimate the total background count rate in detectors in orbit around Mars, it is sufficient to multiply the measured values of the count rate in the apocenter by the K_{SA} coefficient for the altitude of the TGO orbit (see line 2 of Table 3).

Estimates of the full count rate of the detectors in the orbit after making the necessary adjustments to the date of May 2, 2018 are presented in Table 3 (line 3). After subtracting from these values the background count rates estimates (line 2), the average neutron count rate from Mars C_{sig} is obtained (line 4).

C_{sig} values are the end result of FRD processing to obtain the final calibrated FCD/EN and FCD/FN data "product". Statistical errors in the Mars neutron counting rate are determined by the original measurement statistics of C_{tot}, since the errors of the correction and background C_{bgd} coefficients are negligible. These values are estimated on the data of much larger statistics. Possible systematic errors arising from the application of data processing procedures can be validated against independent measurements in near-Martian orbit and ground-based calibrations.

6 Quality control of the obtained FCD calibrated data

6.1 Mean latitudinal flux variability profiles of epithermal and fast neutrons measured in the FREND and HEND experiments

To check the correctness of the procedures of normalization and separation into "signal" and "background" described in the previous chapter, it is necessary to compare the FCD data obtained as a result of processing with the data of other independent measurements or experiments.

Such an experiment is HEND, which has been working in orbit of Mars onboard the Mars Odyssey SC (Mitrofanov et al., 2002) for more than 20 years. The HEND experiment is a suitable candidate for comparison, since it uses similar proportional neutron detectors based on [3]He, it has a similar measurement

methodology and same data format. The main distinction of the HEND instrument is the absence of a collimation module: its viewing angle is limited exclusively by the horizon at the height of the SC orbit, and the spatial resolution is about 600 km (Maurice et al., 2011). In order to compare the data of these two instruments, it is sufficient to average the data of the FREND instrument to the scales corresponding to this spatial resolution.

One can use the averaged latitudinal variability profiles of epithermal and fast neutron fluxes as dataset for comparison, which are obtained after averaging the original global maps by latitudes. To construct latitudinal curves, the FREND and HEND data obtained between May 1, 2018 and November 4, 2021 are averaged within the latitudinal bands of 5°. The resulting graphs are normalized to their own integral at latitudes from 40 ° south to 40° north. Such normalization allows to conveniently compare the graphs of the two instruments. Figure 11 below shows the latitudinal belts that are deposited along the X-axis, and the normalized count values for this band are plotted along the Y-axis.
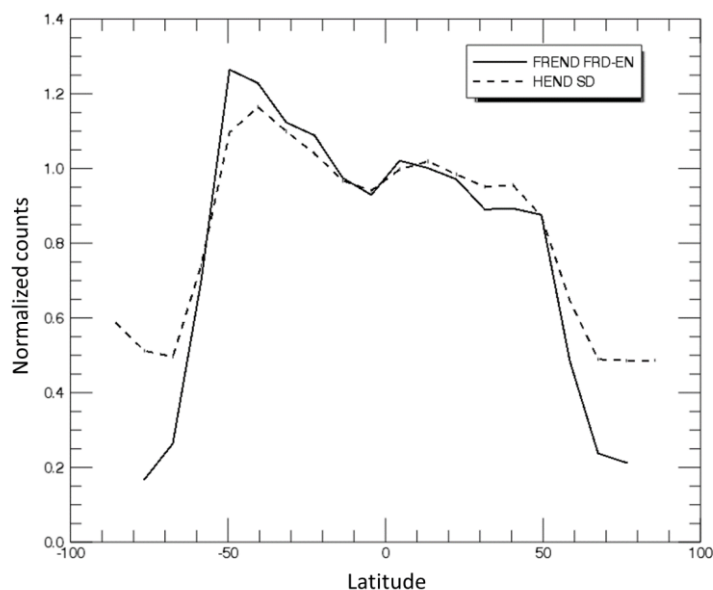

Figure 11 The latitudinal curves of the epithermal detectors of FREND (FRD/EN) and HEND (SD) show good agreement, which indicates the correctness of the described adjustments of the FREND data. The higher count rate of HEND in the polar regions is explained by the spatial resolution of HEND, where there drier regions closer to the equator are seen in the field of view even at these latitudes

A similar comparison was made for the averaged latitudinal profiles of fast neutrons flux, built on the measurement data of the FREND and HEND instruments (Fig. 12).
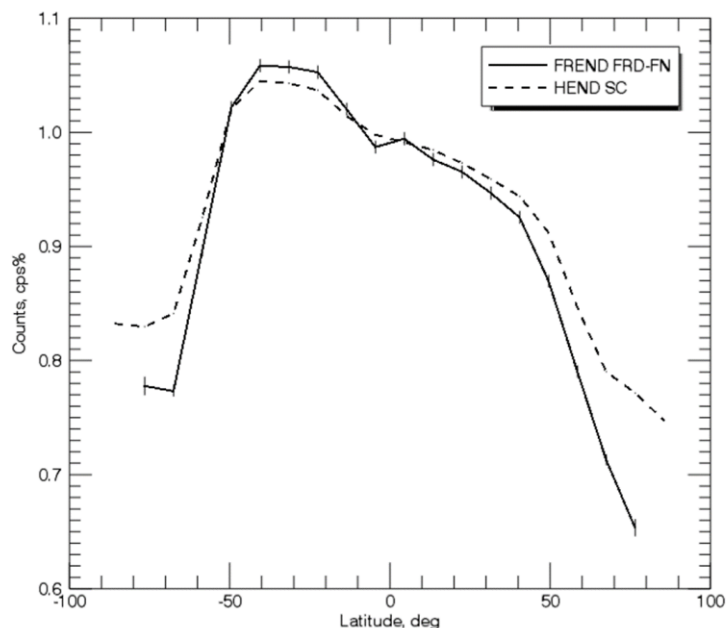
Figure 12 The latitudinal curves of fast neutrons of FREND (FRD/FN) and HEND (SC) show good agreement, which indicates the correctness of the described adjustments of the FREND data. The higher count rate of HEND in the polar regions is explained similarly to Fig. 11

It can be seen that the FREND and HEND curves repeat each other well within the equatorial band from 40 ° N to 40 ° S. In the figure with latitudinal curves, the data are limited to the longitude of 74 ° at both poles due to the inclination of the orbit of the TGO satellite.

7 Conclusion

The processing described in the document make it possible to switch from the initial counts in the detectors of the DSEN and DSFN modules of the instrument to the count rate of the neutron signal from Mars for fixed observation conditions (orbit height, spacecraft orientation, GCR flux). For this purpose, time intervals were selected with favorable observational conditions, corrections were made to take into account the variable efficiency of the detectors, and the data were normalized to exclude variability from GCR flux variations. A signal characterizing the variability of epithermal and fast neutron fluxes from the surface of Mars was extracted from the full count rate.

These signals in the form of time profiles with 5-second time resolution and a reference to Universal Time contain neutron count rate of the HE2-HE4 detectors of the DSEN module and SC detector of the DSFN module, for GCRs with a constant intensity corresponding to the date of May 2, 2018. The resulting data are the official first processing level FCD/EN and FCD/FN "products" of the FREND instrument for the ESA Archive.

These data can be easily plotted on a map of Mars by correlating the measurement time contained for each data item of the product with the spacecraft location above the surface of the planet, available through the publicly available SPICE library(naif.jpl.nasa.gov) and data on the position of the TGO (spice.esa.int). The resulting maps will contain data on the variability of the neutron albedo of Mars on the surface, which is a sign of increased or decreased water content in the regolith. These data are the starting point to obtain a map of the water abundance in the upper layer of the planet's surface. The transition from neutron count rate maps to water abundance maps requires additional assumptions about the nature of the variability of the water mass fraction by depth and carrying out numerical simulation of the entire physical processes

from neutron generation in the planet's substance up to their registration by the FREND instrument detectors. This final stage of the analysis of the experimental data will be described in future documents, simultaneously with the preparation of the corresponding FDD data "product" for the Archive.

The FCD/EN and FCD/FN data processing procedures of the FREND instrument were verified by comparison with the HEND instrument data obtained simultaneously on board of Mars Odyssey orbiter. This comparison confirmed a good agreement of the data with similar spatial resolution scales. At the same time, the use of the FREND data for small spatial resolution scales, corresponding to its field of view, showed that these data make it possible to successfully solve the main task of the experiment - the search and study of local geomorphological areas on Mars with a high water content (Mitrofanov et al., 2022a; Malakhov et al., 2020)

References

Malakhov, A. V., Mitrofanov, I. G., Litvak, M. L., Sanin, A. B., Golovin, D. V., Dyachkova, M. V. ''Oases'' of icy permafrost near the equator of Mars: neutron mapping of the planet according to the FREND instrument on board the TGO satellite of the Russian-European project "ExoMars". Letters to the Astronomical Journal: Astronomy and Space Astrophysics, 2020, No. 46 (06), 1–16. https://doi.org/10.31857/s0320010820060078

Malakhov, A. V., Mitrofanov, I. G., Litvak, M. L., Sanin, A. B., Golovin, D. V., Dyachkova, M. V. Physical calibrations of the neutron telescope FREND installed on board the Martian satellite TGO. Space Research, 2022, No. 60(1), 26–42. https://doi.org/10.31857/S0023420622010095

Boynton, W. M., Feldman, W.C., Squyres, S. W., Prettyman, T. H., Brückner, J., Evans, L. G. Distribution of hydrogen in the near surface of Mars: Evidence for subsurface ice deposits. Science, 2002, №297(5578), 81–85. https://doi.org/10.1126/science.1073722

Drake, D.M., Feldman, W.C., & Jakosky, B.M. Martian neutron leakage spectra. Journal of Geophysical Research, 1988, №93(B6), 6353. https://doi.org/10.1029/jb093ib06p06353

Feldman, W.C., Boynton, W. v., Tokar, R. L., Prettyman, T. H., Gasnault, O., Squyres, S. W. Global distribution of neutrons from Mars: Results from Mars Odyssey. Science, 2002, №297(5578), 75–78. https://doi.org/10.1126/science.1073541

Litvak, M. L., Mitrofanov, I. G., Sanin, A.B., Golovin, D. V., Malakhov, A. V., Boynton, W. V., et al. LEND neutron data processing for the mapping of the Moon. Journal of Geophysical Research E: Planets, 2012, №117(11). https://doi.org/10.1029/2011JE004035

Masarik, J., & Reedy, R.C. Gamma ray production and transport in Mars. Journal of Geophysical Research: Planets, 1996, №101(E8), 18891–18912. https://doi.org/10.1029/96JE01563

MauFig, S., Feldman, W., Diez, B., Gasnault, O., Lawrence, D. J., Pathare, A., & Prettyman, T. Mars Odyssey neutron data: 1. Data processing and models of water-equivalent-hydrogen distribution. Journal of Geophysical Research: Planets, 2011, №116(E11), 11008. https://doi.org/10.1029/2011JE003810

Metzger, A. E., Parker, R. E., & Trombka, J. I. A nondispersive X-ray spectrometer for lunar and planetary geochemical analysis. IEEE Transactions on Nuclear Science, 1966, №NS-13(1), 554–561. https://doi.org/10.1109/TNS.1966.4324015

Mitrofanov, I., Anfimov, D., Kozyrev, A., Litvak, M., Sanin, A., Tret'yakov, V., et al. Maps of Subsurface Hydrogen from the High Energy Neutron Detector, Mars Odyssey. Science, 2002, №297(5578), 78–81. https://doi.org/10.1126/science.1073616

Mitrofanov, I. G., Sanin, A.B., Boynton, W. V., Chin, G., Garvin, J.B., Golovin, D., et al. Hydrogen mapping of the lunar south pole using the LRO neutron detector experiment LEND. Science, 2010, №330(6003). https://doi.org/10.1126/science.1185696

Mitrofanov, I., Malakhov, A., Bakhtin, B., Golovin, D., Kozyrev, A., Litvak, M., et al. Fine Resolution Epithermal Neutron Detector (FREND) Onboard the ExoMars Trace Gas Orbiter. Space Science Reviews, 2018, №214(5). https://doi.org/10.1007/s11214-018-0522-5

Mitrofanov, I., Malakhov, A., Djachkova, M., Golovin, D., Litvak, M., Mokrousov, M., et al. The evidence for unusually high hydrogen abundances in the central part of Valles Marineris on Mars. Icarus, 2022a, №374, 114805. https://doi.org/10.1016/J.ICARUS.2021.114805

Mitrofanov I. G., Sanin A.B., Malakhov A. V., Litvak M. L., Golovin D. V. Numerical modeling of mapping of Marian epithermal neutron emission: applications to FREND investigation onboard ESA's Trace Gas Orbiter, 2022b, Nuclear Instruments and Methods in Physics Research, in press.

Sanin, A.B., Mitrofanov, I. G., Litvak, M. L., Malakhov, A., Boynton, W. V., Chin, G., et al. Testing lunar permanently shadowed regions for water ice: LEND results from LRO. Journal of Geophysical Research E: Planets, 2012, №117(6). https://doi.org/10.1029/2011JE003971

Sanin, A.B., Mitrofanov, I. G., Litvak, M. L., Bakhtin, B. N., Bodnarik, J. G., Boynton, W. V., et al. Hydrogen distribution in the lunar polar regions. Icarus, 2017, 283. https://doi.org/10.1016/j.icarus.2016.06.002

Trombka, J. I., Senftle, F., & Schmadebeck, R. Neutron radiative capture methods for surface elemental analysis. Nuclear Instruments and Methods, 1970, №87(1), 37–43. https://doi.org/10.1016/0029-554X(70)90880-3

Vago, J., Witasse, O., Svedhem, H., Baglioni, P., Haldemann, A., Gianfiglio, G., et al. ESA ExoMars program: The next step in exploring Mars. Solar System Research, 2015, №49(7), 518–528. https://doi.org/10.1134/S0038094615070199